SEMARAK ILMU PUBLISHING

Journal of Advanced Research in Fluid Mechanics and Thermal Sciences

Journal homepage:
https://semarakilmu.com.my/journals/index.php/fluid_mechanics_thermal_sciences/index
ISSN: 2289-7879

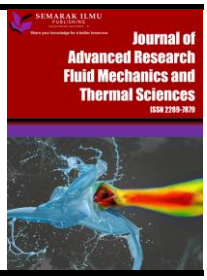

Deployment of Design Sequence for Crossflow Turbine Functionality Enhancement

Williams Saturday Ebhota[1,*], Pavel Yaroslavovich Tabakov[1]

[1] Department of Mechanical Engineering, Durban University of Technology, Durban, South Africa

ARTICLE INFO

Article history:
Received 15 October 2022
Received in revised form 1 February 2023
Accepted 10 February 2023
Available online 24 February 2023

Keywords:
Crossflow turbine; small hydropower (SHP); renewable energy; runner; hydro turbine design

ABSTRACT

The grossly untapped hydro potential in the global south is attributed to the inadequate technical personnel; as one of the main factors limiting the design and manufacturing of efficient small hydropower (SHP) turbine plants. The technical personnel and production facilities available in the global south, especially in sub-Saharan Africa (SSA), cannot support the development of these components sufficiently. The study presents the CFT design process in a clearer and simplified manner. To bridge the technical knowledge gap, the study presents an improved SHP system design procedure through a partly isolated-based design sequence. The entire design process of the SHP turbine, with a focus on crossflow turbine (CFT), was divided into sections, subsections, and parts. The study presents connections between geometry, operation, and functionality of design parameters for CFT components, such as runner, shaft, pulley, and belt graphically and in tabular forms.

1. Introduction

The power situation in developing countries, especially in Sub-Saharan Africa (SSA) and Asia is characterised by inadequate and unreliable supply. This region accommodates the highest population without access to electricity globally and this ugly state, which has been projected to linger on even after 2030, affects the rural areas more and limits economic growth. Ironically, SSA is endowed with vast small hydropower (SHP) potential sites that are inadequately harnessed [1,2]. Adequate tapping of the 3,421 MW estimated SHP (0.1-1 MW) potential sites in SSA can change the region's poor narrative of power supply [3-6]. China has demonstrated the significance of SHP by generating about 19,000 MW of electricity from 43,000 SHP sites. The situation is different from the SSA experience, as the manufacturing facilities and technical personnel in the SSA are grossly inadequate to support such massive power generation projects [7,8]. Many years of SHP exploitation deploying turbines has revolutionised the system to be a reliable source of dependable, cheap, and clean electricity to meet the energy need and studies have shown that the SHP electrification scheme is effective for rural and stand-alone clean electricity systems [9-13]. This energy generation

* *Corresponding author.*
E-mail address: ebhotawilliams1@gmail.com

https://doi.org/10.37934/arfmts.103.2.118140

technology is considered for its design, operation and maintenance simplicity, low cost, and no CO_2 emission. This power system has been tested and is a reliable source of green energy [14-22].

In an SHP system, the hydro turbine is used to convert the hydraulic power in flowing water to electricity. Hydro turbine technology has evolved over the years into different types, such as Pelton, Turgo, crossflow (CFT), and Francis turbines and their applications depend on the head. In the context of the head, hydropower turbines are categorised into three groups [23,24]: high, medium, and low head. The propeller, CFT, and Kaplan turbines are the three commonest low-head turbines; multi-jet Pelton, CFT and Turgo turbines are used for the medium head; and Pelton, Turgo, multi-jet Pelton turbines are applied for the high head. Because of CFT's simplicity and low costs compared to other turbine types, CFT is mostly applied in low-head sites while the Pelton turbine is considered for high-head sites. Other merits and limitations of CLT are presented in Table 1.

Table 1
Merits and demerits of CLT relative to other hydro turbines [25,26]

Advantages	Disadvantages
Relatively cheap to design and fabrication	Problems for self-starting
CLT has good regulations	Its performance coefficient reduces
Low-cost maintenance and simple operation process	The maximum efficiency of the cross-flow turbine is slightly lower than the maximum efficiency of the Pelton, Francis, and Kaplan turbines
CLT is more dependable in low heads compared to other types	It makes a relatively loud noise during the operation
The efficiency is high when the water flows through the impeller twice	
Reliable in micro and small hydroelectric applications	
CLT design and fabrication are relatively simple	
CLT has better annual efficiency generated	
For mini-run, water power plants, CLT has the best annual efficiency generated by the flat efficiency curve compared to other turbine types	

The different turbine maintains distinct efficiency profiles, as shown in Figure 1, with CFT having a range of 70–85%. Pelton Turbine is one the most efficient turbines (about 90%) and sustains the optimum efficiency for a varying range of flows. Crossflow turbine sustain optimum efficiency levels for a range and possesses relatively inferior efficiency levels. However, CFT is the commonest applied SHP turbine in developing countries because of its fabrication simplicity and low-cost investment. Other advantages of CFT include less maintenance, long service life, and being economically and environmentally friendly [27].

In the global south, the exploitation and development of the SHP system are faced with many drawbacks, which include a lack of access to appropriate SHP turbine technologies and inadequate technical personnel [7,29,30]. Studies have strived to bridge the identified technical gaps through the adoption of different design and fabrication methods and models and several of these studies failed in terms of simplicity and clarity, computation reliability, and detail [31-34]. Because of the importance of the SHP system in increasing clean electricity access and reducing GHG emissions, all hands should on the desk to develop the vastly SHP sites for electricity. Hence, this study addresses the gap in the design of the CFT mechanical unit, comprising of the runner, nozzle, and power transmission parts, such as shaft, belt, and pulley. The relative CFT's design and production simplicity and low-costs is the reason for the choice of the type of turbine considered in this study. The study

targets to provoke greater rural participation in the design and manufacture of CFT components and systems in the global south.

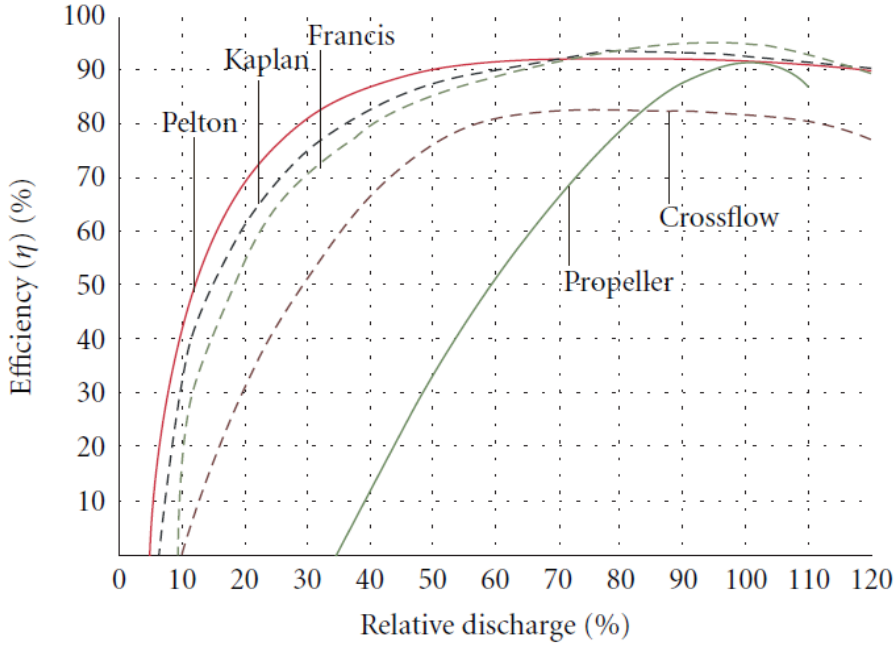

Fig. 1. The efficiency curves for the different hydropower turbines [28]

The study involves the establishment of correlations between geometry, operation, and functional design parameters, as well as simplifying design computation; considering optimization values for CFT design for manufacturing (DFM). Getting the right information during the design process is cumbersome, requires a lot of effort and is time-consuming. Hence, this study focuses on simplifying the design of an efficient CFT to make it precise by tabulating and graphically representing the CLT design process sequence. This will present the theoretical, manufacturing, and operation relations and conditions between CLT parameters and components at glance. This is aimed at reducing the time and cost of production by prioritizing the ease of designing for manufacturing CFT mechanical components.

1.1 Understanding the Hydropower System

The utilisation of renewable energy (RE) in developing countries will reduce the negative environmental impact of fossil fuels and other non-renewable energy sources, as well as increase the population that has access to clean electricity. The energy in flowing water, called hydropower is one of the RE sources that are commonly known and used as a form of alternative energy. Other RE sources present in the energy matrix of various countries in SSA are wind, solar, geothermal, and biomass.

1.2 Hydroelectricity: Energy Conversion and Small Hydropower

Hydropower (hydroelectric power), is the generation of electricity from the alternator, driven by a turbine that converts the hydraulic potential energy of flowing or falling water, into mechanical energy, which equals the differential net head. The energy in the flowing water is associated with natural gravity as in the case of waterfalls, shown in Figure 2(a). Besides, in the case of large hydropower, this energy can be boosted artificially through topographic waterfalls in rivers or

through hydraulic conveyance systems, as shown in Figure 2(b). Small hydropower utilizes either water that runs off a river, diversion from a river, or a waterfall that uses natural elevation drop without a dam; and it is devoid of negative environmental impacts.

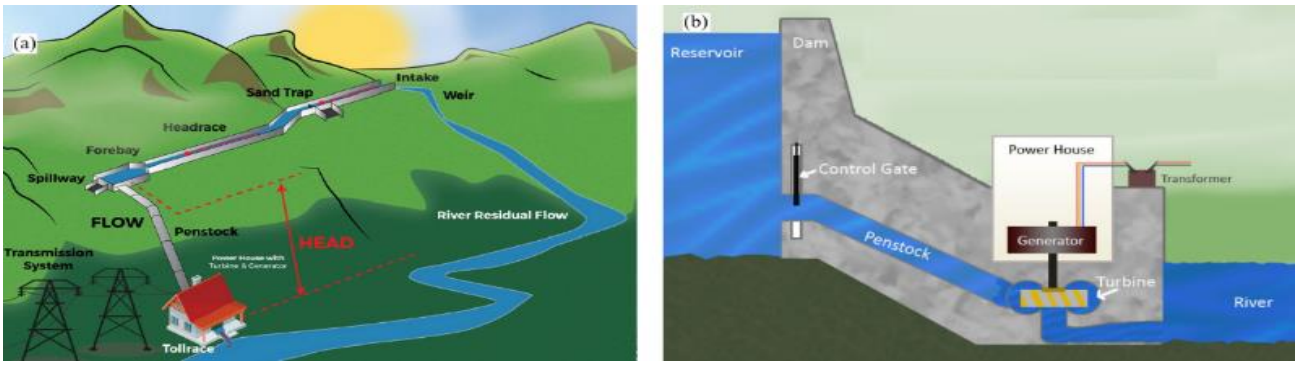

Fig. 2. propagation of energy in a flow-through: (a) natural gravity [35]; and (b) artificially created topographic waterfalls [36]

1.3 Classification of Small Hydropower Plant

Hydro turbines are broadly grouped into two – reaction and impulse turbines. In the reaction turbines, the spinning wheel is completely immersed in the flow and is usually deployed for low and medium-head sites [4,8]. Impulse turbines involve the conversion of high-pressure flow into jets of water that possess high velocity and kinetic energy by passing the water through a nozzle at atmospheric pressure. The generated high-speed jets of water with kinetic energy impinges on a turbine blade and this exerts an impulsive force on the runner making it spin. This type of turbine has three main sub-types in use - the Turgo, the Pelton, and the crossflow/Banki turbines.

Further, SHP classification can be based on installed capacity, although, there are no internationally acceptable standardized classification at present [37]. Some countries and organizations have classified hydropower based on capacity, as presented in Figure 3 and Table 2 [5,38]. However, many international energy organizations regard SHP as a plant with an installed capacity of not more than 10 MW. In China and India SHPs with an installed capacity of not more than 50 MW and 25 MW, respectively [39].

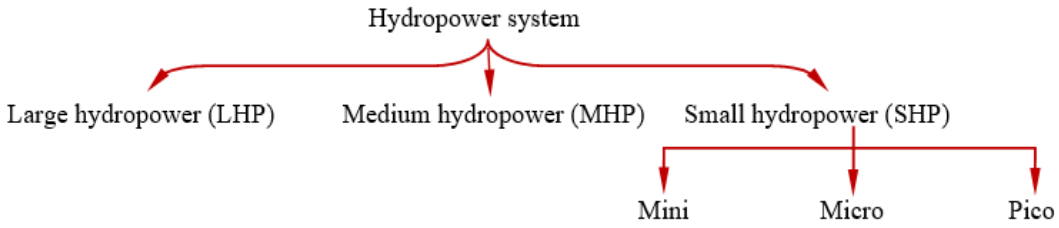

Fig. 3. Hydropower system classification based on generation scale

According to the United Nations Industrial Development Organization (UNIDO), the International Association for Small Hydro (IASH), and the European Small Hydropower Association (ESHA), a capacity of 10 MW and below is referred to as small hydropower plants (SHP) [40].

Table 2
Classification of SHP [41]

Class	Size	Area of application
Mini (MH)	Less than 1 MW	Grid connection
Micro	Less than 100 kW	Partially grid connection
Pico (PH)	Less than 10 kW	Offgrid
Family (FH)	Less than ~1 kW	Standalone/single households

1.4 Renewable Energy Domestic Capacity Building

Two extreme realities exist in SSA – a region endowed with untapped SHP potential sites and other RE resources [42-44]; a region with the highest population without access to adequate power. How best can one correlate these statements, apart from being contradictory? A scenario of living in energy poverty amid abundant untapped RE resources; the estimate of the region's technical generation RE potential is 11,000 GW [44]. These RE resources are in the form of exploitable permanent streams and rivers for SHP, and only about 7% of these sites in Africa have been tapped [45]. The RE natural resources underutilisation deficiency of SSA is attributed to the passive participation of the region in the design and manufacturing of RE components, devices, and systems. This translates to insufficient participation of SSA in the promotion of access to affordable, adequate, and clean electricity to meet the power required to stimulate socio-economic growth. The region's passiveness is responsible for the insufficiency of RE-skilled personnel and the manufacturing process of RE components and systems and making SSA a consuming region. Unless the principle of self-dependency is imbibed, the region's power infrastructure will continue to be vulnerable to overdependence on foreign technology and expertise. Because dependency comes with the consequences of the high cost of power projects, installation, maintenance, operation, and repair challenges and creates barriers to domestic RE technologies development.

Therefore, it is imperative to develop domestic capacity in the design, manufacturing, and management of RE components, devices, and systems for sustainable energy delivery in the region. China is a perfect example of the significance of having adequate skilled personnel and manufacturing capacities in the development and deployment of RE technologies domestically. Domestic capacity development of RE technologies facilitates substantial reduction of cost of RE projects, operations, and maintenance and downtime. A deliberate capability building in emerging technologies and their applications in the RE sector is required to expedite domestic participation and sustainable adequate power delivery in SSA. Such emerging areas include fluid mechanics, foundry technology, manufacturing processes, material science and engineering, and mechatronics.

This study presents the CFT design process in a clearer and simplified way by partly isolated-based design sequence to bridge the existing technical knowledge gap in the SHP system design. The entire design process of the SHP turbine will be classified into sections, subsections, and components. The connections between geometry, operation, and functionality of design parameters for CFT components, such as runner, shaft, pulley, and belt will be represented graphically and in tabular forms.

2. Methodology

The design and production of a hydro turbine plant follow a systemic pattern, which begins with a hydrological study and ends with project commissioning. The entire design and production process is categorized into two components– civil work and turbine mechanical design. This study focuses on the development of design sequence layouts of mechanical components of CFT. To improve the CFT

design process's clarity and simplicity, partly isolated-based design sequence models were developed; interlinks between geometry, operation, and functionality design parameters layouts were represented graphically; and the relevant design expressions for sizing and selecting each of the parts in isolated basis were established. The objectives of this study are as follows

i. Classification of the mechanical component into units and graphical representation of the links between these units.
ii. The identified units will further be stratified into subunits and their design parameters and relationships interlinked graphically based on optimisation conditions.
iii. Mathematical equations for designing a CFT runner and optimization conditions of the design and operation parameters were considered and tabulated.
iv. Item iii was repeated for the major units and parts of the mechanical component of CFT, such as the shaft, pulley, and belt.

3. Small Hydropower Design, Fabrication, and Deployment of CFT

In the development of an SHP site for power generation, the CFT is usually deployed in a low head because of its relative efficiency, simplicity, and low cost to design, fabricate, and operate [46]. The application of CFTs is frequently used in remote power systems in the Global South and typically, its efficiency is in the range of 70–85%. Despite the efficiency being lower than other types, the CFT exhibits a flatter efficiency curve with varying runner angular velocity, ω, which can be a crucial added advantage. Since its invention by Michell in 1903, more is still being done to improve its maximum efficiency, $\eta_{max,}$ and manufacturability. The CFT is deployed within a head range of 1-100 m and is an impulse type of turbine that can power up to 221 kW. The speed is a function of the runner's diameter and the head and is operated from 60-2000 RPM. The recommended average annual flows for CFTs are between 0.04 m^3/s to 5 m^3/s; other turbines are applied at higher flow rates. The locally fabricated micro and macro complex CFTs are between 60-75% and as high as 85%, respectively [47].

The Crossflow and Pelton turbines belong to the same family of a turbine, the impulse turbine but different heads application; Pelton and CFT turbines are used for high and low heads, respectively. The following components form the basic electromechanical units of a CFT system regulator (generator controller), alternator or generator, and transmitting wiring unit. The turbine operates on the principle of converting the hydraulic energy in flowing water to a rotary motion that turns the alternator via a shaft to generate electricity. The CFT consists of the following units − nozzle, runner, and transmitting parts (belt, pulley, and shaft). Other parts include the bearing, casing, guide vane, air valve, and draft tube as shown in Figure 4.

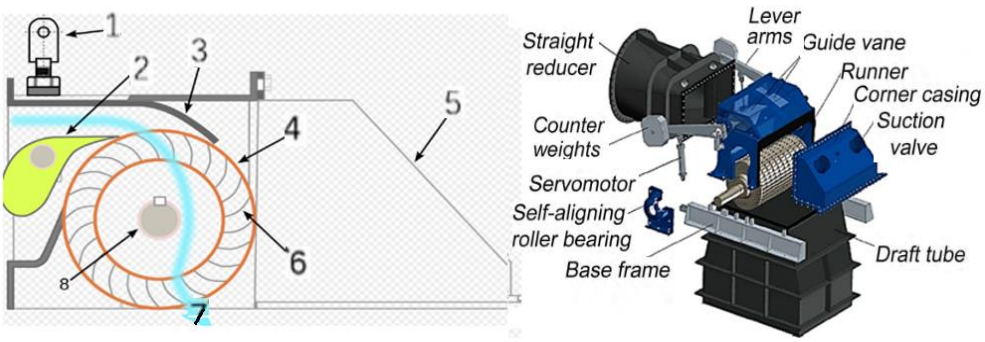

Note: 1-air-venting valve, 2-guide vane, 3-nozzle, 4-runner, 5-removable rear casing, 6-blades, 7-water flow, and 8-shaft

Fig. 4. The components of the original OSSBERGER cross-flow turbine [48,49]

3.1 Systematic Design of CFT System

The systematic design process sequence of CFT begins with the SHP site's hydrological properties including sizing parameters and information, such as the runner's nozzle and blade, shaft, and transmission belt, as represented diagrammatically in Figure 5.

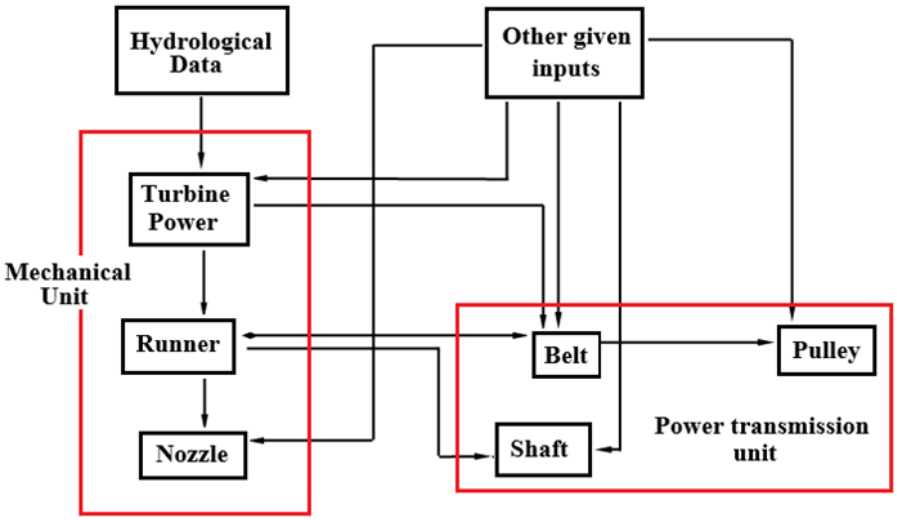

Fig. 5. Schematic diagram of CFT mechanical components design interlinks

The determination of fabrication and operation parameters of a CFT runner requires the mathematical equations presented in Table 3.

Table 3
The required mathematical expressions to design a CFT runner

Runner		
V_1 (m/s) is the runner's velocity before it enters the water.	$V_1 = C(2gH_n)^{1/2}$	The coefficient of velocity, C, provides for the losses through the nozzle. The value is between 0.92 and 0.99 but less than 1
U_1 (m/s) is the runner's tangential velocity	$U_1 = 0.5V_1 \cos\alpha$ $= \frac{\pi DoN}{60}$	Maximum efficiency, η_{max}, depends on the wheel periphery velocity, U_1, which is about $0.5V_1$. But η_{max} occurs when the value of U_1 is about $0.46V_1$ empirically
k_u is the coefficient of rotational velocity	$k_u = \frac{U_1}{V_1}$	Where k_u is from 0.4 to 0.5
V_{rt} (m/s) is the runner's outer diameter rotational velocity	$V_{rt} = 1/2 * C * \sqrt{2 * g * H_n}$	
TSR is the tip speed ratio	$TSR = \frac{r_o \omega}{V_1}$	Where r_o is the runner radius (m) while V_1 is the runner inlet velocity (m/s)
D_o (m) is the outer diameter	$D_o = 39.85\frac{\sqrt{H}}{N}$	
D_i (m) is the runner's wheel inner diameter	$D_i = 0.66D_o$	D_i/D_o is about 0.66 [50]
a (m) is the runner tangential spacing or radial rim width	$a = 0.174D_o$ $= r_o - r_i$	
L (m) is the turbine runner length	$L = \frac{QN}{50H}$	

Blade design		
β_1 (°) is the outer blade angle in	$tan\beta_1 = 2 * tan\alpha$ $\beta_1 = \tan^{-1}(2 * \tan\alpha)$	
β_2 (°) is the inner blade angle	$\beta_2 = \frac{\pi}{2} = 90°$	When radial flow is perfect i.e., having the operating fluid flowing mostly along the rotation radii
λ (°) is the inlet discharge angle	$\lambda = 90^o$	Empirical studies have shown that the performance of the crossflow is influenced by the inlet discharge angle influences and 90° is usually recommended to 120° [51]
δ (°) is the blade central angle	$\delta = 2\tan^{-1}\left(\frac{\cos(\beta_1)}{\left(\sin(\beta_1)+\frac{r_i}{r_o}\right)}\right)$	The blade central angle aids the realization of the crossflow process. This is the angle between the outer sides and the blade's inner. The blade position on the rims relies on δ
r_b (m) is the radius of the blade	$r_b = 0.326r_o$	
r_p (m) is the pitch circle diameter in	$r_p = 2r_b$	
t_e (m) is the Blade jet entrance	$t_e = kD_o$	
s (m) is the blade spacing.	$s = \frac{kD_o}{\sin\beta_1}$	The value of k is between 0.075 and 0.1. The water strikes the blades optimally for maximum thrust production to occur. This requires the spacing of the blades reasonably. The number of blades on the runner determines the spacing.
	$s = 0.174D_o$	When k = 0.87, β_1 = 30° and α = 16°.
n is the number of blades	$n = \frac{\pi D_o}{s}$	Experimental studies have revealed that the number of blades for optimisation is 24 to 30. Fewer blades cause pulsating power, otherwise, excessive friction losses occur
n_E is the effective blade's number	$n_E = \frac{\pi D_o}{s} + (0.3n)$	The performance of CFT is affected by the number of blades and studies have shown that the addition of at least 30% of the calculated value is more effective [52-54]

The general systematic interconnectivity of parameters required in the design of the CFT system is depicted in Figure 6. This procedural process generates the design values to fabricate the runner, nozzle, blade, belt, and shaft. However, the sequential process can be isolated based on the parts and focus of the study. The CFT deployment gained acceptance because of the simplicity of its design, fabrication, and maintenance, and the possibility of a wide range of operational heads (4 to 200 m) and discharge (0.04 to 5 m^3/s).

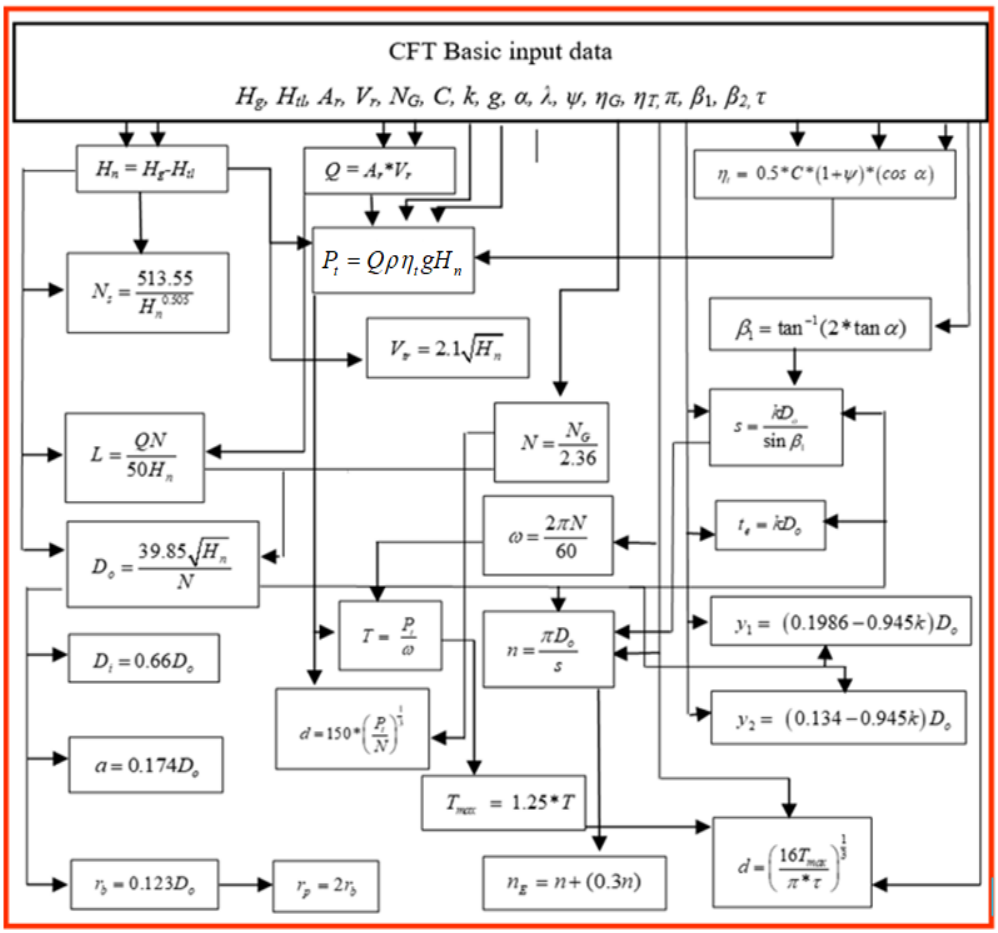

Fig. 6. Systematic procedure of CFT system design

3.1.1 The runner

The component of a CFT that converts the hydraulic energy possessed by the water jets received from the nozzle into a rotary motion, is a cylindrical rotor, called a runner. The hydraulic performance and speed of CFT are influenced by the size of the runner's diameter. A Crossflow turbine is classified as a small turbine if its diameters are between 200-500 mm. The composition of a runner is presented in Figure 7.

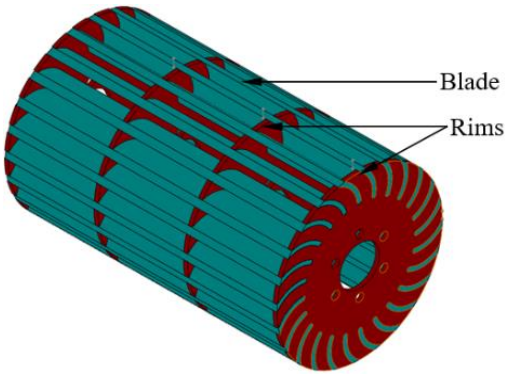

Fig. 7. CFT runner

3.1.2 The number of rims and blades

The number of rims depends on the length of the runner, and the minimum for a very short runner is two. The rim is deployed to place the blades at two defined angles, outer (β_1) and inner angles (β_2), and for bracing as structural support. The geometrical parameters and 3-dimensional view are represented in Figure 8(a) and (b), respectively.

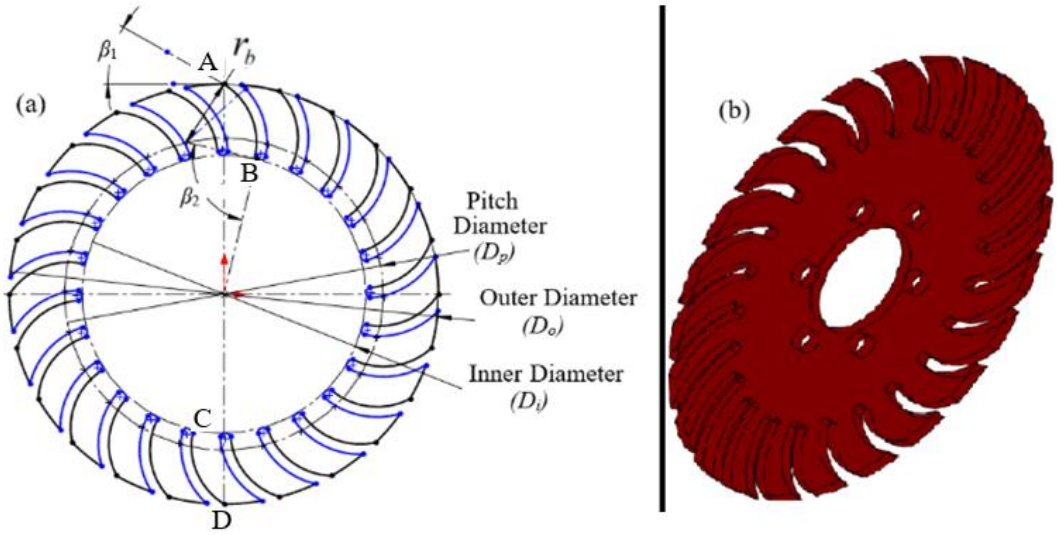

Fig. 8. CFT rim (a) geometrical parameters; (b) 3-D form

The CFT blades are circular arcs with a small thickness and are uniquely arrayed at an angle on parallel discs (rims), as shown in Figure 9. The CFT is designed in such a way that the flow passes twice through the rotating runner. The nozzle is the first entry point of the flow and then moves through the air-space centre and exits through the second stage.

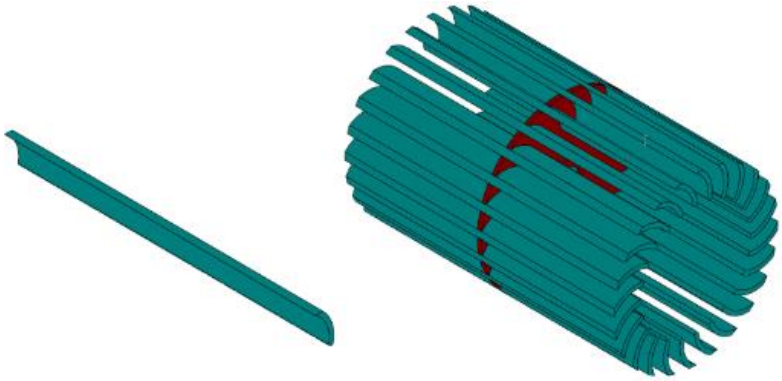

Fig. 9. CFT circular blades

One of the significant considerations in the design of a runner is the determination of the optimum number of blades. Studies have shown that the first stage does not transform all the available energy into power [55,56]. The squirrel-cage blower form of CFT enables the water to flow across the blades twice. Considering Figure 9, in the first stage, the waterjet enters the runner at point A to strike blade, AB, tangentially and then flows across the empty space to the inner side of the runner at point C. In the second stage, the water, again, hits the blade, CD, and discharges through the outer, D. Literature has divergent views on the blade of CFT in terms of number and angle [57-59]. Too many blades increase a runner's loss, weight, and cost while too few blades cause

incomplete utilization of water [60]. This prompted several studies to verify the effects of many blades on CFT performance. Many of these studies came up with 24 to 30 as the optimum number of blades [47,61]. However, some experimental studies recommend that a minimum of 30% of the calculated number of blades should be added [52-54]. This is mathematically expressed in the equation defining the number of effective blades (n_E) presented in Table 3. A good design process can address the hydraulic flow and structural requirements challenge sufficiently. This study presents the design process sequence for CFT, as shown in Figure 10. The construction of a runner requires the following parameters inner diameter (D_i), outer diameter (D_o), blade spacing (S), number of blades (N), pitch diameter (D_p), blade radius (r_b), and outer blade angle (β_1). It includes inner blade angle (β_2), pitch radius (r_p), central blade angle (δ), inner radius to outer radius ratio (r_o/r_i), radial rim width (a), and attack angle (α) [62].

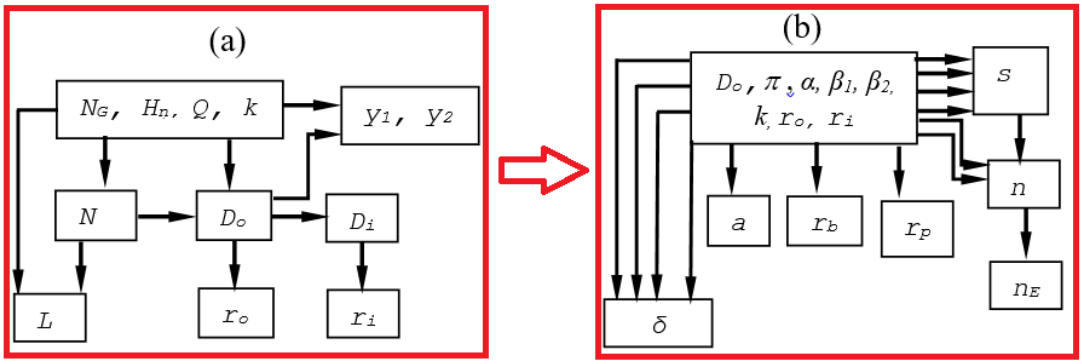

Fig. 10. (a) Defines the size of a runner; (b) displays blade design process sequence for fabrication parameters

3.1.3 The nozzle

The runner and rectangular nozzle of a CFT have the same width. Based on the head, the nozzle transports and converts flowing water into a water jet directed towards the blades of the runner at an angle called the angle of attack (α). The kinetic energy in the water jet causes the runner to spin about its axis with minimal energy loss. The construction parameters for the nozzle, runner, and other key CFT components, are presented in Figure 11.

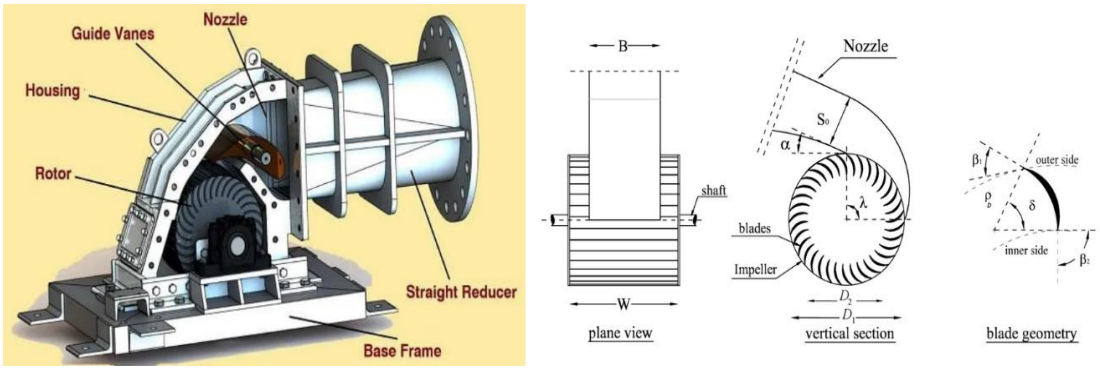

Fig. 11. Features and key geometrical parameters of CFT [62,63]

The efficiency of a CFT is influenced by the geometry of the runner and nozzle. The inlet or attack angle of a water jet to the outer blades differs. Attack angle is a significant parameter in CFT nozzle design and studies have shown that the optimum value of α is normally from 16° - 25° [50,64,65]. The nozzle transforms a calculated amount of running water into water jets and channels it to the

runner at a certain angle, as depicted in Figure 12(a). The sequence of the CFT nozzle design process is presented in Figure 12(b).

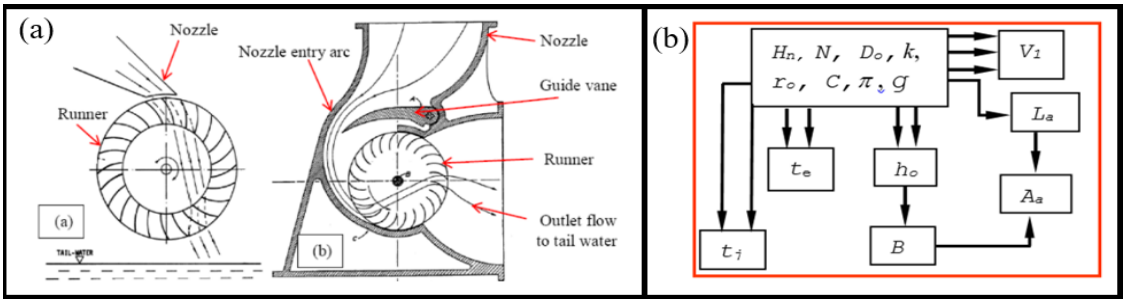

Fig. 12. The CFT (a) runner and nozzle [53]; (b) the sequence of the design process of the CFT nozzle

The required mathematical expressions to design, and fabricate a CFT nozzle are presented in Table 4.

Table 4
Mathematical expressions for CFT nozzle design

Nozzle		
α is the attack angle (°)	α = 16° to 25°	
y_1 (m) is the jet distance from the centre of the shaft	$y_1 = (0.1986 - 0.945k)D_o$	Where k = 0.087
y_2 (m) is the jet distance from the inner periphery of the wheel	$y_2 = (0.134 - 0.945k)D_o$	Where k = 0.087
h_o (m) is the nozzle throat	$\frac{B}{h_o} = 1.5$	B is the nozzle width
T_r is the nozzle throat width ratio	$T_r = \frac{2h_o}{D_o\lambda} = \sin\alpha$	λ is the admittance angle
h_o (m) is the thickness of the jet	$h_o = 0.17D_o$ $h_o = \frac{Area\ of\ jet(A)}{Nozzle\ width} = \frac{Q/V_1}{B}$ $Q = AV_1 = h_oLC\sqrt{2gH_n}$	Jet thickness, h_o, is about 0.1 to 0.2 times D_o
L_1 (m) is the real length	$L_1 = L + 0.1L$	The runner's actual length is L plus 10% more [50,60].
Runner length and diameter ratio	$0.16 < \frac{L_1}{D_o} \geq \frac{21.24}{H^{0.85}}$	
A (m²) is the area of the jet	$A = \frac{Q}{V_1} = h_oB$	
A_a (m²) is the area of admission flow	$A_a = b_aL_a$	b_a *is* the inlet width
L_a (m) is the admission arc length	$L_a = \frac{2r_o\pi\lambda}{360}$ *if* $\lambda = 90°$ $= \frac{1}{2}r_o\pi$	λ° is the admission arc L_a angle

3.2 The Transmission Subsystem

The rotating machine elements, such as the shaft, pulley, and belt that form the transmission subsystem, are responsible for the transmission of the hydraulic power harnessed by the runner of CFT to the alternator that generates electricity.

3.2.1 The shaft

Amongst the rotating elements of CFT, the shaft is the most critical. Usually, a shaft is a solid or hollow machine element with a circular cross-section. The runner and other transmission elements in a CFT are mounted on the shaft and then linked to the alternator by a belt (V or flat). Besides the transmission of power, the shaft houses the belt pulley, and the runner and its components. The parts that make the runner are circular blades and a minimum of two rims, depending on the length of the runner. The shaft is always supported by ball bearings at both sides of the runner, as shown in Figure 13.

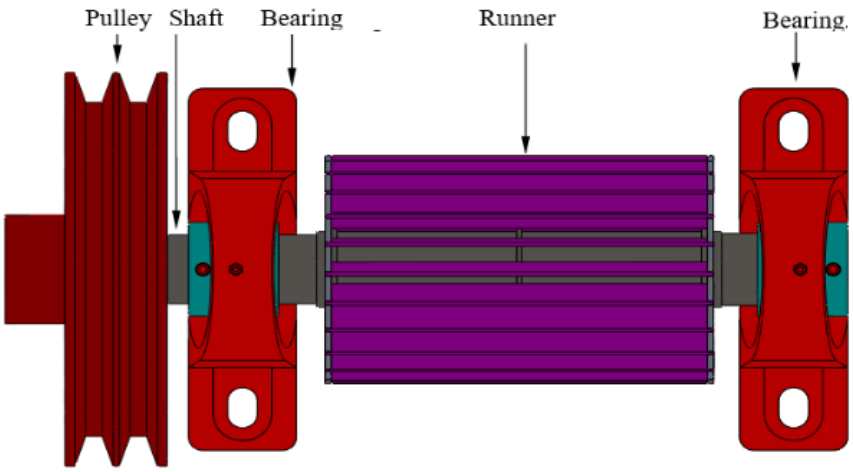

Fig. 13. A schematic of a runner and shaft supported by two ball bearings

Strength and rigidity are the two most vital attributes the shaft requires to transmit power under a loading system and operating conditions satisfactorily. At a given rotational speed, the resulting power-transmitting process subjects the CFT shaft to a torque or torsional moment and bending. The shaft is mostly subjected to a steady torsion during constant rotation with the bending stresses completely reversed. Because CFT shafts are mostly fabricated from ductile materials, the maximum shear stress theory is deployed during design. To control a satisfactory performance and to prevent the shaft from deflecting more than 1 degree, its length of it should be 20 times its diameter. The estimation of the minimum dimension of a shaft's diameter that can withstand the maximum torque generated during operation is a requirement to avoid failure. The mathematical expressions required to determine the minimum shaft dimension without failure, and sequence of the design process are presented in Table 5 and Figure 14, respectively.

Table 5
Mathematical relations for shaft design

Turbine shaft design and stress analysis		
Turbine's theoretical shaft power (P_s) (W)	$P_s = \left(\frac{\omega Q U_1}{g}\right)(V_1 \cos\alpha_1)\left(1+\frac{C\cos\beta_2}{\cos\beta_1}\right) = \omega T$	The empirical friction effect coefficient is C and is taken as 0.98, less than unity while the angular speed of the shaft in radians is ω
The shaft angular speed (ω) in radians	$\omega = \frac{2\pi N}{60}$	
Power of the turbine (P_t)	$P_t = T * \omega$	
Torque of the turbine shaft (T)	$T = \frac{P_t}{\omega}$	
The maximum torque (T_{max}) in N-m	$T_{max} = 1.25 * T = \frac{\pi * d^3 \tau}{16}$	The turbine shaft diameter is d; shaft material shear stress (τ) for steel = 42 MPa
Turbine shaft diameter (d) in m	$d = \left(\frac{16 T_{max}}{\pi * \tau}\right)^{\frac{1}{3}}$	The allowable stress for a shaft under a simple torsional moment; $\tau = (0.5-0.577)\sigma_y$
The rotational velocity of the runner's outer diameter, V_{rt} (m/s)	$V_{rt} = 1/2 * C * \sqrt{2 * g * H_n}$	
The relation in an open belt drive system; power transmission to the alternator unit,	$\frac{N_2}{N_G} = \frac{d_G}{d_s}$	The diameters of the driver and driven pulleys are d_G and d_s, respectively, while the speeds of the driver and driven pulleys *are* N_G and N.
The turbine theoretical efficiency (η_o)	$\eta_o = \frac{Shaft\ power}{Water\ power}$	
The shaft diameter, d (m)	$d = 150 * \left(\frac{P_t}{N}\right)^{\frac{1}{3}}$	

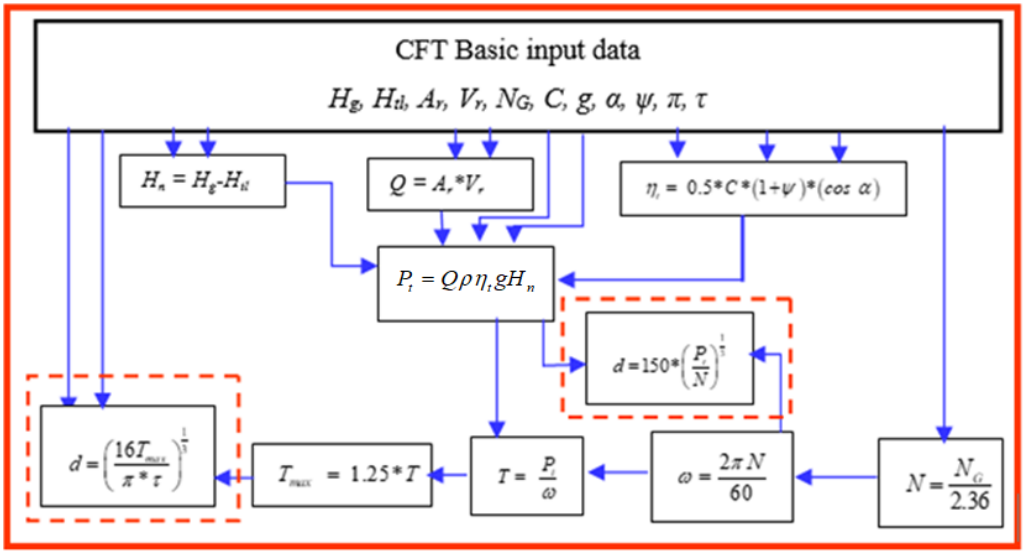

Fig. 14. The design process sequence to compute CFT shaft diameter

3.2.1.1 Shaft material selection

Carbon steel materials of about 0.1 to 0.33% carbon, such as AISI 1045, 1060, 52100, and 1566, account for around 85% of all shafts used in industrial automation. The materials' relative attributes

of low cost, easy machinability and hardenability make them outstanding shaft materials. However, these materials fail at certain harsh working conditions, such as elevated temperatures and the notorious medium turbine works with rapid corrosion. The turbine shaft sometimes works in a saline water medium and in this scenario, a shaft of carbon steel will likely underperform due to rapid corrosion. The alloy steel shafts of compositions of aluminium, silicon, copper, and stainless steel offer varying degrees of corrosion resistance and strength and are considered and deployed for performance better. Other alloying elements that are used to enhance stainless steel are manganese, silicon, aluminium, copper, titanium, sulphur, nickel, niobium, selenium, and molybdenum [66,67]. The best option for shaft materials, offering high corrosion resistance and strength is stainless steel, which exploits the combination of low carbon content and chromium of not less than 12%. The 300 and 400-series stainless steel (austenitic steel), such as 304, 316, and 430, which contain about 16 to 25% chromium are the commonly used stainless steel for shaft fabrication [68]. In this study, AISI 1045 steel of yield Strength 530 N/mm^2 was selected as the shaft material with a consideration of 2.5 as a minimum factor of safety (FOS) was seen as satisfactory. Table 6 presents the physical properties of AISI 1045 steel.

Table 6
Physical properties of AISI 1045 steel

Name	Cold-drawn AISI 1045 steel
Type of model	Linear Elastic Isotropic
Yield strength (N/m^2)	5.3e+08
Tensile strength (N/m^2)	6.25e+08
Elastic modulus (N/m^2)	2.05e+11
Poisson's ratio	0.29
Mass density (kg/m^3)	7850
Shear modulus (N/^{m2})	8e+10
Thermal expansion coefficient (Kelvin^-1)	1.2e-05

3.2.2 V-Belt selection

Generally, a power transmission or friction drive belt utilises friction between the pulley and belt to transmit power from one point to another. This concept of mechanical power transmission has been deployed for several years, providing drive solutions to different industries and applications. There are three main types - flat, round, and V-belts and certain factors determine the choice of belt type to use. These factors include - speed, positive-drive requirements, centre distances, shaft correlation, and reduction ratio. The V-belts have the operational advantage of the wedging action provided by the V-shape and this makes it an effective mechanical constant power transmission means commonly used in industrial and automobile applications. They are used in automobile engines to drive accessories, such as the power steering pump, air conditioning compressor, cooling fan, and alternator. The V-belt a loop of flexible material is used to link two or more rotating parallel shafts via pulleys mechanically. It has a trapezoidal cross-sectional area, a shape that allows it to align with the pulleys. This geometry increases the low tensioning force to amplify the frictional force on the pulley sidewalls. In addition, V-belt is relatively low in cost, has ease of installation, and has a wide range of sizes. There are three fundamental components of a V-belt, as shown in Figure 15 – (1) belt body, made of a special rubber; (2) tensile member body, entailing high-strength low-stretch cords; and (3) fabric cover or jacket made of fabric, protecting the tensile member.

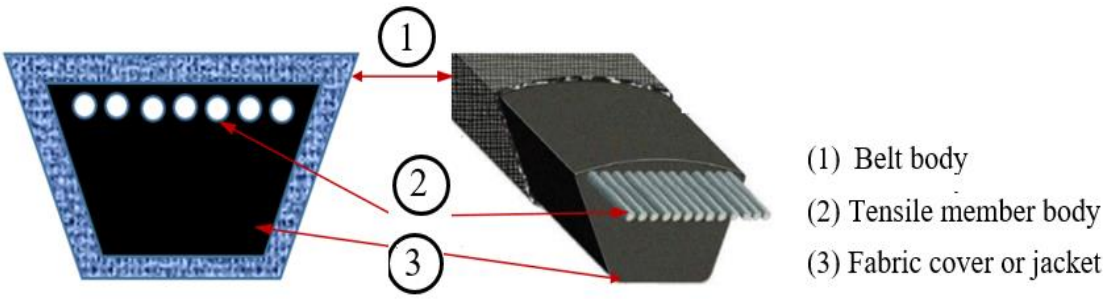

Fig. 15. Cross-section of a V-belt, showing it main components

In a CFT, a V-belt links two pulleys: the shaft pulley (runner section), which serves as a driver, and the alternator pulley (generating section), the driven. This concept is used to transmit motion from the runner unit of CFT to the alternator. During operation, the V-belt optimal speed is 20 m/s at a drive speed of not more than 30 m/s. The features, geometry, parameters, and profile of a V-belt and pulley based on general considerations are shown in Figure 16.

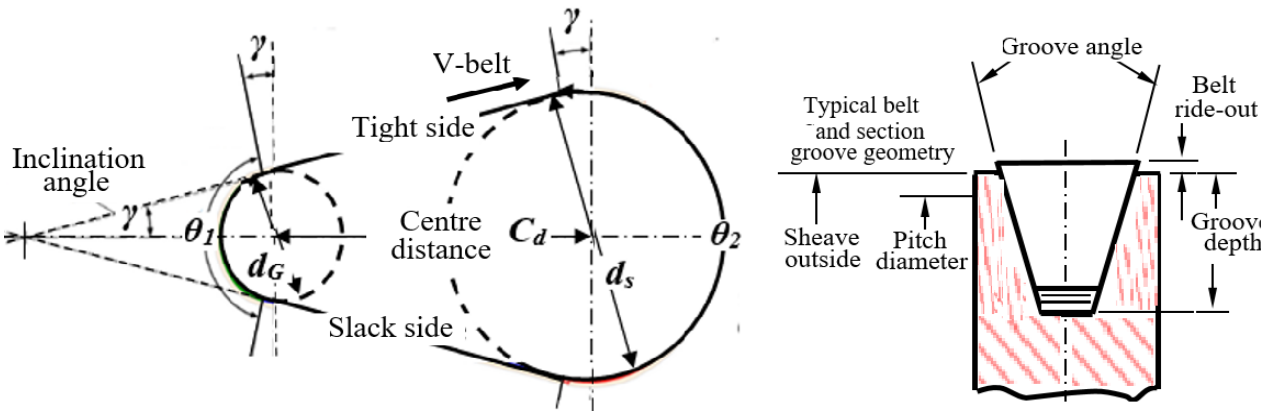

Fig. 16. Transmission belt-pulleys and V-belt cross-sectional area

The mathematical expressions and sequence of steps required for the design and selection of the V-belt and pulley are shown in Table 7 and Figure 17, respectively.

V-belt comes in different section standards applied for a range of power transmission capacities, and these sections are represented by A, B, C, D and E, as shown in Table 8. The section of the V-belt to be used depends on the capacity of power being transmitted and this has nothing to do with the number of belts. The economic significance controls belt selection in the case of falling transmitting power within the overlapping zone.

Table 7
The expressions for V-belt and pulley design

V-belt and pulley design		
Transmission ratio (R_t) $R_t \geq 1$	$R_t = \frac{N_G}{N} = \frac{d_{sp}}{d_{Gp}}$	Where d_{Gp} and d_{sp} are the driving pulley pitch diameter and the driven pulley pitch diameter, respectively.
Belt datum length (L_{dL}) in mm	$L_{dL} = 2*C_{dd} + 1.57*(d_s + d_G)$	Where C_{dd} is the centre distance of the belt drive in mm: $0.7*(d_s + d_G) < C_{dd} < 2*(d_s + d_G)$
Belt centre distance (C_d) in mm	$C_d = C_{dd} - \frac{(L_{dL} - L_{dLs})}{2}$	Where L_{dLs} is the belt datum's actual standard length. It was picked from DIN 2215/ISO 4184 standard range table based on the estimated and the centre distance, C_d L_{dL} $d_s < C_d < 3(d_s + d_G)$
The belt length (L_B) in mm	$L_B = 2*C_d + \frac{pi*(d_s + d_G)}{2} + \frac{(d_s - d_G)^2}{(4*C_d)}$	
Wrap angle ($\vartheta°$)	$\gamma = \sin^{-1}\left(\frac{d_s - d_G}{2L_B}\right)$ $\theta_1 = 180 - 2\gamma$ $\theta_2 = 180 + 2\gamma$	Where ϑ_1, ϑ_2, and γ are generator pulley contact, shaft pulley contact, and inclination angles, respectively.
Design power (P_{des})	$P_{des} = C_{serv}P_t$	Where C_{serv} is the service factor, which depends on service conditions, such as light, medium, heavy or extra-heavy-duty, driven machinery and type of driver, and operational hours. The value of C_{serv} is from 1 to 1.8.
Corrected power rating (P_{cor})	$P_{cor} = P_R K_{length} K_a$	Where P_R is the power rating for the transmission; and K_a is the contact factor.
Belt speed, V_{belt}	$V_{belt} = \frac{d_G N_G}{19100}$	
Number of belts (B_N)	$N_B = \frac{P_{des}}{P_{cor}}$	
Belt flex rate (F_b) in s^{-1}	$F_b = 2*1000*\frac{V_{belt}}{L_{dLs}}$	

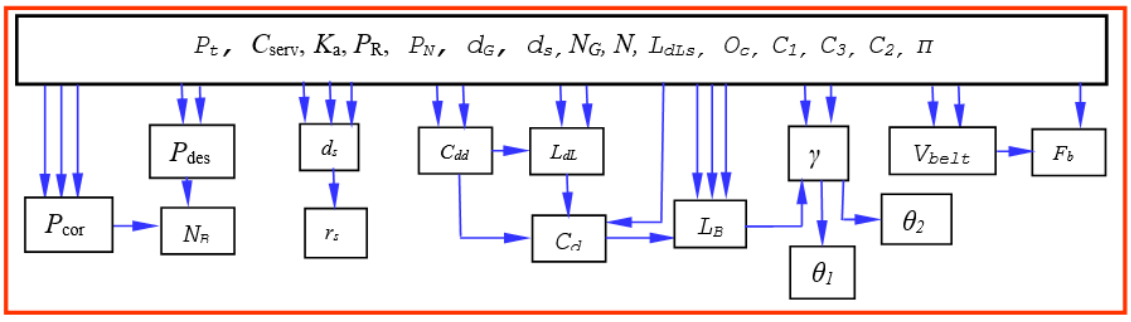

Fig. 17. Sequence of V-belt design and selection process

Table 8
V-belt section standards [69-71]

Section	Power range (kW)	Width (mm)	Thickness (mm)	Minimum pulley pitch diameter (mm)
A	0.4 – 4	13	8	125
B	1.5 - 15	17	11	200
C	10 - 70	22	14	300
D	35 - 150	32	19	500
E	70 - 260	38 - 40	23 - 25	630

3.2.3 The pulley

A pulley is a wheel fixed on the axle or shaft, devised to transfer power between two or more parallel shafts connected with a belt or cable. There are two types of pulleys, as shown in Figure 18 – V-belt pulleys (with groove), as in Figure 18(a) and flat pulleys (without grooves), as in Figure 18(b). Other driving elements for a pulley system apart from a belt are rope, cable, and chain.

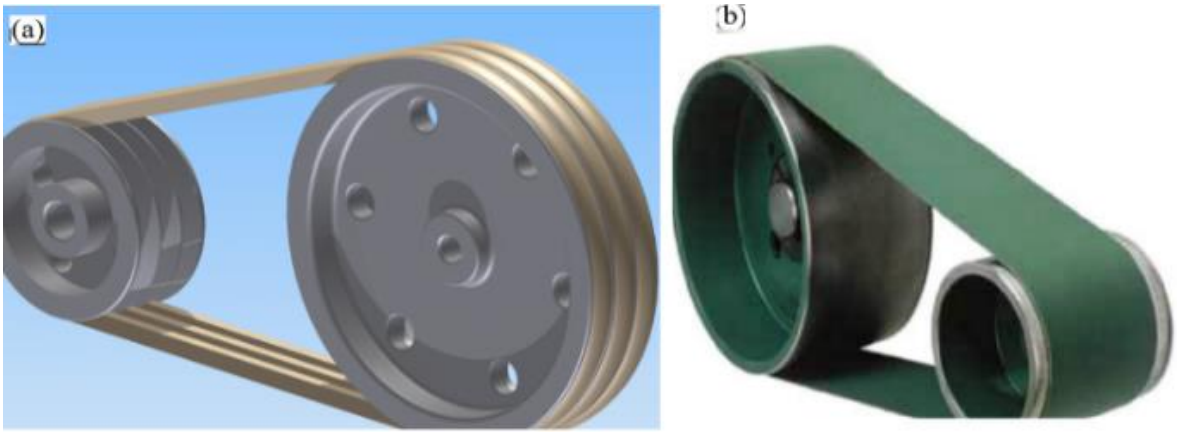

Fig. 18. Pulley - (a) V-belt and pulleys; (b) flat belt and pulleys

In-built features, such as machined grooves, aid V-belt pulleys to maximise their grips on the shaft, and they are commonly fabricated from graded cast iron and mild steel. The profile and features of a normal V-belt pulley conforming to the selected V-belt section are depicted in Figure 19.

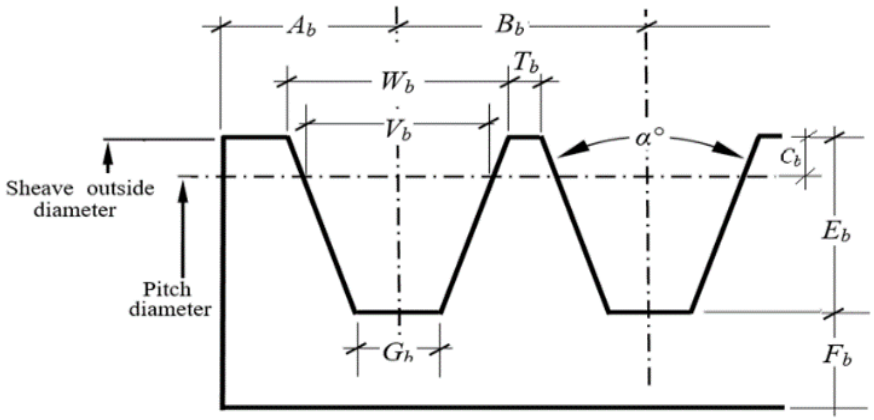

Fig. 19. A profile of standard V-belt sheave grooves

As the belt rides in the pulley, the pitch pulley diameter (P.D) represents the belt's diameter and section D of the standards of the V-belt section, is the most suitable for a turbine capacity of 112.4 kW under consideration. The V-belt section standards are presented in Table 9. The design and selection parameters of the standard V- belt, section D, are presented in Table 9.

Table 9
V-belt section D - standard dimensions and sheave grooves

A_b (mm)	B_b (mm)	C_b (mm)	D_b (mm)	E_b (mm)	V_b (mm)	T_b (mm)	G_b (mm)	W_b (mm)	Groove angle (α°)	Used pitch datum (mm)
3.2	30.2	7.6	7.6	26.7	27.3	4.5	20.6	32.0	34	317.5
						4.2	15.0	32.3	36	381
						4.0	14.0	32.6	38	508

4. Hydropower Outlooks and the Deployment of CLT

The global market for hydropower generation is increasing, mainly driven by the demand for a reliable and adequate supply of green electricity to meet industrialisation and urbanisation. An increase in the energy supply-demand gap is a prime concern for utilities in the global south and this requires significant investments to substantially develop sustainable power generation sources such as hydropower. According to Research and Market report in 2019, the value of the global hydropower generation market was at $202.4 billion with a projection of $317.8 billion by 2027 [72]. However, there are divergent views about large hydropower (LHP) plants because of environmental issues caused by the large volume of water involved and its negative impacts along the coastal areas. Consequently, the global hydropower generation market has been categorised based on capacity into three sizes - SHP plant (up to 1MW), medium hydropower (MHP) plant (1MW-10MW), and LHP plant (above 10MW). This coupled with the highly capital-intensive required for LHP projects, favours the deployment of SHP turbines, especially in the global south, such as SSA. The SSA has the highest percentage of untapped hydropower potential and people without access to electricity [42]. The estimated technical potential of identified SHP potential sites across the sub-continent is 15,599 and this opens varied market opportunities considering SHP design, development, and deployment paths of the value chain.

5. Conclusions

The power perennial problem of SSA has so far negated efforts to change the energy narrative of the region. This is further confronted by climate change and the global quest for a global sustainable energy supply adequate. Through the instrumentalities of the UN, a declaration for cheap, adequate, and clean energy for all by 2030 has been made. The inability of SSA to adequately exploit the abundant SHP resources for a steady and sufficient power supply in the region is attributed to the lack of technical personnel in terms of design and fabrication, and strong manufacturing infrastructure. Hence, this study is presented to bridge the identified gap through academic-based SHP turbine capacity building to facilitate domestic participation in the design and development of CFT. To achieve this goal, the study considered a collection of established optimization conditions in a simplified design process of CFT. The paper is designed to serve as a CFT design and construction guide and it includes the correlations between geometry, operation, functionality, and design parameters of the runner, nozzle, and power transmission parts, such as shaft, belt, and pulley.

In the future, energy usage is already seen by studies that are going to be higher despite the level of improvement reached in energy efficiency. The quest for renewable energy in place of fossil energy

will complicate the entire scenario. The deployment of hydro turbines in the generation of green electricity will increase in areas with SHP potential sites. To meet this need, the capacity to design and manufacture SHP plants, such as CFT, and increase local participation in the global south desires to be developed.

Acknowledgement
The authors hereby acknowledge the Research and Postgraduate Support Directorate, Institute for Systems Science, and the Management of Durban University of Technology, South Africa, for their continuous support.

References

[1] Ebhota, Williams S. "Power accessibility, fossil fuel and the exploitation of small hydropower technology in sub-saharan Africa." *International Journal of Sustainable Energy Planning and Management* 19 (2019): 13-28.
[2] Ebhota, Williams S., and P. Y. Tabakov. "Power Supply and the Role Hydropower Plays in Sub-Saharan Africa's Modern Energy System and Socioeconomic Wellbeing." *International Journal of Energy Economics and Policy* 9, no. 2 (2019): 347-363.
[3] Korkovelos, Alexandros, Dimitrios Mentis, Shahid Hussain Siyal, Christopher Arderne, Holger Rogner, Morgan Bazilian, Mark Howells, Hylke Beck, and Ad De Roo. "A geospatial assessment of small-scale hydropower potential in Sub-Saharan Africa." *Energies* 11, no. 11 (2018): 3100. https://doi.org/10.3390/en11113100
[4] Ebhota, Williams S., and Freddie Inambao. "Design basics of a small hydro turbine plant for capacity building in sub-Saharan Africa." *African Journal of Science, Technology, Innovation and Development* 8, no. 1 (2016): 111-120. https://doi.org/10.1080/20421338.2015.1128039
[5] Ebhota, Williams S., and Freddie L. Inambao. "Facilitating greater energy access in rural and remote areas of sub-Saharan Africa: Small hydropower." *Energy & Environment* 28, no. 3 (2017): 316-329. https://doi.org/10.1177/0958305X16686448
[6] Ebhota, Williams S., and Freddie L. Inambao. "Smart design and development of a small hydropower system and exploitation of locally sourced material for pelton turbine bucket production." *Iranian Journal of Science and Technology, Transactions of Mechanical Engineering* 43 (2019): 291-314. https://doi.org/10.1007/s40997-017-0134-9
[7] Ebhota, Williams S., and Freddie L. Inambao. "Electricity insufficiency in Africa: A product of inadequate manufacturing capacity." *African Journal of Science, Technology, Innovation and Development* 8, no. 2 (2016): 197-204. https://doi.org/10.1080/20421338.2016.1147206
[8] Ebhota, Williams, and Pavel Y. Tabakov. "Hydropower Potentials and Effects of Poor Manufacturing Infrastructure on Small Hydropower Development in Sub-Saharan Africa." *International Journal of Energy Economics and Policy* 7, no. 5 (2017): 60-67.
[9] Obadote, D. J. "Energy crisis in Nigeria: technical issues and solutions." In *Power Sector Prayer Conference*, vol. 23, no. 10, pp. 25-27. 2009.
[10] Klein, S. J. W., and E. L. B. Fox. "A review of small hydropower performance and cost." *Renewable and Sustainable Energy Reviews* 169 (2022): 112898. https://doi.org/10.1016/j.rser.2022.112898
[11] Lai, Rouyi, Xiaohong Chen, and Lilan Zhang. "Evaluating the impacts of small cascade hydropower from a perspective of stream health that integrates eco-environmental and hydrological values." *Journal of Environmental Management* 305 (2022): 114366. https://doi.org/10.1016/j.jenvman.2021.114366
[12] Shiji, Chu, Sagar Dhakal, and Chuanqi Ou. "Greening small hydropower: A brief review." *Energy Strategy Reviews* 36 (2021): 100676. https://doi.org/10.1016/j.esr.2021.100676
[13] Ugwu, Collins O., Paul A. Ozor, and C. Mbohwa. "Small hydropower as a source of clean and local energy in Nigeria: Prospects and challenges." *Fuel Communications* 10 (2022): 100046. https://doi.org/10.1016/j.jfueco.2021.100046
[14] Arias-Gaviria, Jessica, Bob van der Zwaan, Tom Kober, and Santiago Arango-Aramburo. "The prospects for small hydropower in Colombia." *Renewable Energy* 107 (2017): 204-214. https://doi.org/10.1016/j.renene.2017.01.054
[15] Breeze, Paul. "Chapter 6 - Small Hydropower." *Hydropower* (2018): 53-62. https://doi.org/10.1016/B978-0-12-812906-7.00006-5
[16] Breeze, Paul. "Chapter 5 - Hydropower Generators." *Hydropower* (2018): 47-52. https://doi.org/10.1016/B978-0-12-812906-7.00005-3
[17] Harlan, Tyler. "Rural utility to low-carbon industry: Small hydropower and the industrialization of renewable energy in China." *Geoforum* 95 (2018): 59-69. https://doi.org/10.1016/j.geoforum.2018.06.025

[18] Ioannidou, Christina, and Jesse R. O'Hanley. "Eco-friendly location of small hydropower." *European Journal of Operational Research* 264, no. 3 (2018): 907-918. https://doi.org/10.1016/j.ejor.2016.06.067
[19] Khodayar, Mohammad E. "Rural electrification and expansion planning of off-grid microgrids." *The Electricity Journal* 30, no. 4 (2017): 68-74. https://doi.org/10.1016/j.tej.2017.04.004
[20] Kong, Yigang, Jie Wang, Zhigang Kong, Furong Song, Zhiqi Liu, and Congmei Wei. "Small hydropower in China: The survey and sustainable future." *Renewable and Sustainable Energy Reviews* 48 (2015): 425-433. https://doi.org/10.1016/j.rser.2015.04.036
[21] Li, Xiao-zhu, Zhi-jun Chen, Xiao-chao Fan, and Zhi-jiang Cheng. "Hydropower development situation and prospects in China." *Renewable and Sustainable Energy Reviews* 82 (2018): 232-239. https://doi.org/10.1016/j.rser.2017.08.090
[22] Pang, Mingyue, Lixiao Zhang, AbuBakr S. Bahaj, Kaipeng Xu, Yan Hao, and Changbo Wang. "Small hydropower development in Tibet: Insight from a survey in Nagqu Prefecture." *Renewable and Sustainable Energy Reviews* 81 (2018): 3032-3040. https://doi.org/10.1016/j.rser.2017.06.115
[23] Williamson, Sam J., Bernard H. Stark, and Julian D. Booker. "Low head pico hydro turbine selection using a multi-criteria analysis." *Renewable Energy* 61 (2014): 43-50. https://doi.org/10.1016/j.renene.2012.06.020
[24] Khattak, M. A., N. S. Mohd Ali, N. H. Zainal Abidin, N. S. Azhar, and M. H. Omar. "Common Type of Turbines in Power Plant: A Review." *Journal of Advanced Research in Applied Sciences and Engineering Technology* 3, no. 1 (2016): 77-100.
[25] CINK. "Crossflow turbines." *CINK Hydro-Energy* (2022). https://www.cink-hydro-energy.com/crossflow-turbines.
[26] Engineer Waqar. "What is a Crossflow Turbine? | How does a Cross-flow Turbine Work?." *Mechanical Boost*. March 9, 2021. https://mechanicalboost.com/crossflow-turbine-an-overview/.
[27] Warjito, Warjito, Budiarso Budiarso, Celine Kevin, Dendy Adanta, and Aji Putro Prakoso. "Computational methods for predicting a pico-hydro crossflow turbine performance." *CFD Letters* 11, no. 12 (2019): 13-20.
[28] Kaunda, Chiyembekezo S., Cuthbert Z. Kimambo, and Torbjorn K. Nielsen. "Potential of small-scale hydropower for electricity generation in Sub-Saharan Africa." *ISRN Renewable Energy* 2012 (2012): 1-15. https://doi.org/10.5402/2012/132606
[29] Sambo, A. S. "Overview of policy landscape in Africa on SHP project development and management." In *International Hydropower Conference, Abuja*. 2008.
[30] Edeoja, A. O., J. S. Ibrahim, and E. I. Kucha. "Suitability of pico-hydropower technology for addressing the Nigerian energy crisis-A review." *International Journal of Engineering Inventions* 4, no. 9 (2015): 17-40.
[31] Dorji, Ugyen, and Reza Ghomashchi. "Hydro turbine failure mechanisms: An overview." *Engineering Failure Analysis* 44 (2014): 136-147. https://doi.org/10.1016/j.engfailanal.2014.04.013
[32] Jayaram, V., and B. Bavanish. "Design and analysis of gorlov helical hydro turbine on index of revolution." *International Journal of Hydrogen Energy* 47, no. 77 (2022): 32804-32821. https://doi.org/10.1016/j.ijhydene.2022.07.181
[33] Rengma, Thochi Seb, and P. M. V. Subbarao. "Optimization of semicircular blade profile of Savonius hydrokinetic turbine using artificial neural network." *Renewable Energy* 200 (2022): 658-673. https://doi.org/10.1016/j.renene.2022.10.021
[34] Titus, Joel, and Bakthavatsalam Ayalur. "Design and fabrication of in-line turbine for pico hydro energy recovery in treated sewage water distribution line." *Energy Procedia* 156 (2019): 133-138. https://doi.org/10.1016/j.egypro.2018.11.117
[35] ASEAN. "Small hydropower in Southeast Asia." *The ASEAN Post*. March 8, 2018. https://theaseanpost.com/article/small-hydropower-southeast-asia.
[36] Daware, Kiran. "Hydroelectric Power Plant: Layout, Working and Types." *Electrical Easy*. Accessed February 25, 2021. https://www.electricaleasy.com/2015/09/hydroelectric-power-plant-layout.html.
[37] Haidar, Ahmed M. A., Mohd F. M. Senan, Abdulhakim Noman, and Taha Radman. "Utilization of pico hydro generation in domestic and commercial loads." *Renewable and Sustainable Energy Reviews* 16, no. 1 (2012): 518-524. https://doi.org/10.1016/j.rser.2011.08.017
[38] Manzano-Agugliaro, Francisco, Myriam Taher, Antonio Zapata-Sierra, Adel Juaidi, and Francisco G. Montoya. "An overview of research and energy evolution for small hydropower in Europe." *Renewable and Sustainable Energy Reviews* 75 (2017): 476-489. https://doi.org/10.1016/j.rser.2016.11.013
[39] Hicks, Charlotte. "Small hydropower in China: A new record in world hydropower development." *Refocus* 5, no. 6 (2004): 36-40. https://doi.org/10.1016/S1471-0846(04)00258-6
[40] IHA. "2020 Hydropower Status Report - Sector trends and insights." *International Hydropower Association, United Kingdom*, 2020. https://hydropower-assets.s3.eu-west-2.amazonaws.com/publications-docs/2020_hydropower_status_report.pdf.

[41] Energypedia. "Hydro Power Basics." *Energypedia*. Accessed March 28, 2017. https://energypedia.info/wiki/Hydro_Power_Basics#cite_note-1.
[42] Ouedraogo, Nadia S. "Africa energy future: Alternative scenarios and their implications for sustainable development strategies." *Energy Policy* 106 (2017): 457-471. https://doi.org/10.1016/j.enpol.2017.03.021
[43] International Energy Agency. "Africa Energy Outlook: A Focus on Energy Prospects in Sub-Saharan Africa." *IEA, London,* 2014. https://www.icafrica.org/en/knowledge-hub/article/africa-energy-outlook-a-focus-on-energy-prospects-in-sub-saharan-africa-263/.
[44] Oxfam. "The energy challenge in sub-Saharan Africa." *Oxfam's Research Backgrounder series, Washington*, 2017. https://www.oxfamamerica.org/explore/research-publications/the-energy-challenge-in-sub-saharan-africa/.
[45] Klunne, Wim Jonker. "Small Hydropower Development in Africa." *ESI Africa*. July 31, 2017. https://www.esi-africa.com/top-stories/small-hydropower-development-in-africa-8038/.
[46] Adejumobi, I. A., A. A. Esan, and A. B. Okunuga. "Discovering Potential Sites for Small Hydro Power (SHP) in Nigeria." In *Advanced Materials Research*, vol. 18, pp. 93-97. Trans Tech Publications Ltd, 2007. https://doi.org/10.4028/www.scientific.net/AMR.18-19.93
[47] Will, S. "Corazón del Bosque Hydroelectric Scheme: engineering design document." *Appriopriate Infrastructure Development Group (AIDG), Guatemala* (2010).
[48] OSSBERGER. "The Original OSSBERGER™ Cross-Flow Turbine." *OSSBERGER GmbH, Weißenburg, Germany*, 2014. http://nebula.wsimg.com/e8abdd247e75fec9cda79df25a13b893?AccessKeyId=99A8DBD7DC79A02F55C8&disposition=0&alloworigin=1.
[49] Wikipedia. "Cross-flow turbine." *Wikimedia Foundation Inc.,* 2021. https://en.wikipedia.org/wiki/Cross-flow_turbine.
[50] Mockmore, Charles Arthur, and Fred Merryfield. "The Banki water turbine." *Technical Report, Oregon State College* (1949).
[51] Fiuzat, Abbas A., and Bhushan P. Akerkar. "Power outputs of two stages of cross-flow turbine." *Journal of Energy Engineering* 117, no. 2 (1991): 57-70. https://doi.org/10.1061/(ASCE)0733-9402(1991)117:2(57)
[52] Ngoma, Daniel H., Yaodong Wang, and Tony Roskilly. "Crossflow turbine design specifications for hhaynu micro-hydropower plant-mbulu, tanzania." *Innovative Energy & Research* 8, no. 2 (2019): 1000225.
[53] Kaunda, Chiyembekezo S., Cuthbert Z. Kimambo, and Torbjorn K. Nielsen. "A numerical investigation of flow profile and performance of a low cost Crossflow turbine." *International Journal of Energy & Environment* 5, no. 3 (2014): 275-296.
[54] Olgun, Hayati. "Effect of interior guide tubes in cross-flow turbine runner on turbine performance." *International Journal of Energy Research* 24, no. 11 (2000): 953-964. https://doi.org/10.1002/1099-114X(200009)24:11<953::AID-ER634>3.0.CO;2-3
[55] Quaranta, Emanuele, Jean Pierre Perrier, and Roberto Revelli. "Optimal design process of crossflow Banki turbines: Literature review and novel expeditious equations." *Ocean Engineering* 257 (2022): 111582. https://doi.org/10.1016/j.oceaneng.2022.111582
[56] Achebe, C. H., O. C. Okafor, and E. N. Obika. "Design and implementation of a crossflow turbine for Pico hydropower electricity generation." *Heliyon* 6, no. 7 (2020): e04523. https://doi.org/10.1016/j.heliyon.2020.e04523
[57] Jiyun, Du, Shen Zhicheng, and Yang Hongxing. "Study on the effects of blades outer angle on the performance of inline cross-flow turbines." *Energy Procedia* 158 (2019): 1039-1045. https://doi.org/10.1016/j.egypro.2019.01.252
[58] Ketata, Ahmed, Zied Driss, and Mohamed Salah Abid. "Impact of blade number on performance, loss and flow characteristics of one mixed flow turbine." *Energy* 203 (2020): 117914. https://doi.org/10.1016/j.energy.2020.117914
[59] Ranjan, Rajeev Kumar, Nur Alom, Jaswant Singh, and Bikash Kumar Sarkar. "Performance investigations of cross flow hydro turbine with the variation of blade and nozzle entry arc angle." *Energy Conversion and Management* 182 (2019): 41-50. https://doi.org/10.1016/j.enconman.2018.12.075
[60] San, Myin, and Nyi Nyi. "Design of cross flow turbine and analysis of runner's dimensions on various head and flow rate." *International Journal of Scientific and Research Publications (IJSRP)* 8, no. 8 (2018): 586-593. https://doi.org/10.29322/IJSRP.8.8.2018.p8076
[61] Du, Jiyun, Zhicheng Shen, and Hongxing Yang. "Study on the effects of runner geometries on the performance of inline cross-flow turbine used in water pipelines." *Sustainable Energy Technologies and Assessments* 40 (2020): 100762. https://doi.org/10.1016/j.seta.2020.100762
[62] Adhikari, Ram, and David Wood. "The design of high efficiency crossflow hydro turbines: A review and extension." *Energies* 11, no. 2 (2018): 267. https://doi.org/10.3390/en11020267
[63] Mehr, Goodarz, Mohammad Durali, Mohammad Hadi Khakrand, and Hadi Hoghooghi. "A novel design and performance optimization methodology for hydraulic Cross-Flow turbines using successive numerical simulations." *Renewable Energy* 169 (2021): 1402-1421. https://doi.org/10.1016/j.renene.2021.01.090

[64] Aziz, Nadim M., and Venkappayya R. Desai. "A laboratory study to improve the efficiency of cross-flow turbines." *Engineering Report* (1993).
[65] Aziz, N. M., and H. G. S. Totapally. "Design Parameter Refinement for Improved Cross Flow Turbine Performance." *Engineering Report* (1994).
[66] Shilun, Zuo, Zhou Xiong, and Zhang Gang. "Comprehensive welding technology for type 304 stainless steel rotating shaft." *Procedia Engineering* 24 (2011): 840-844. https://doi.org/10.1016/j.proeng.2011.11.2747
[67] McGuire, Michael F. *Stainless steels for design engineers*. ASM International, 2008. https://doi.org/10.31399/asm.tb.ssde.9781627082860
[68] Davis, Joseph R., ed. *Alloy digest sourcebook: stainless steels*. ASM international, 2000.
[69] Megadyne. "V-Belts." *Direct Industry*. Accessed February 20, 2021. https://pdf.directindustry.com/pdf/megadyne/v-belts/14254-179437-_8.html.
[70] Bando. "V-Belt Design Manual." *Bando, USA* (2018). https://www.bandousa.com/media/uploads/0/1352_bu-143-V-belt-design-manual_updated-2018.pdf.
[71] Optibelt. "Technical Manual V-Belt Drives." *Optibelt GMBH, Germany* (2021). https://www.optibelt.com/fileadmin/pdf/produkte/keilriemen/Optibelt-TM-v-belt-drives.pdf.
[72] Research and Markets. " Hydropower Generation Market by Capacity, Medium Hydro Power Plant and Large Hydro Power Plant: Global Opportunity Analysis and Industry Forecast, 2020-2027." *Research and Markets, Dublin, Ireland*. January 2021. https://www.researchandmarkets.com/reports/5306416/hydropower-generation-market-by-capacity-medium#tag-pos-14.